1

DEPARTMENTAL REPORT

DETERMINATIONS OF PHOTON SPECTRA

Submitted by

David L. Wannigman
Department of Radiology and Radiation Biology

Academic Advisor
Thomas B. Borak, Ph.D.

In partial fulfillment of the requirements
for the Degree of Master of Science
Colorado State University
Fort Collins, Colorado
Fall 1989

SECURITY CLASSIFICATION OF THIS PAGE

REPORT DOCUMENTATION PAGE

Form Approved
OMB No. 0704-0188

1a. REPORT SECURITY CLASSIFICATION UNCLASSIFIED	1b. RESTRICTIVE MARKINGS NONE
2a. SECURITY CLASSIFICATION AUTHORITY	3. DISTRIBUTION/AVAILABILITY OF REPORT APPROVED FOR PUBLIC RELEASE; DISTRIBUTION UNLIMITED.
2b. DECLASSIFICATION/DOWNGRADING SCHEDULE	
4. PERFORMING ORGANIZATION REPORT NUMBER(S)	5. MONITORING ORGANIZATION REPORT NUMBER(S) AFIT/CI/CIA- 89-152
6a. NAME OF PERFORMING ORGANIZATION AFIT STUDENT AT CO STATE UNIV 6b. OFFICE SYMBOL (If applicable)	7a. NAME OF MONITORING ORGANIZATION AFIT/CIA
6c. ADDRESS (City, State, and ZIP Code)	7b. ADDRESS (City, State, and ZIP Code) Wright-Patterson AFB OH 45433-6583
8a. NAME OF FUNDING/SPONSORING ORGANIZATION 8b. OFFICE SYMBOL (If applicable)	9. PROCUREMENT INSTRUMENT IDENTIFICATION NUMBER
8c. ADDRESS (City, State, and ZIP Code)	10. SOURCE OF FUNDING NUMBERS PROGRAM ELEMENT NO. / PROJECT NO. / TASK NO. / WORK UNIT ACCESSION NO.

11. TITLE (Include Security Classification) (UNCLASSIFIED)
DETERMINATIONS OF PHOTON SPECTRA

12. PERSONAL AUTHOR(S)
THOMAS B. BORAK

13a. TYPE OF REPORT	13b. TIME COVERED	14. DATE OF REPORT (Year, Month, Day)	15. PAGE COUNT
THESIS/DISSERTATION	FROM _____ TO _____	1989	54

16. SUPPLEMENTARY NOTATION
APPROVED FOR PUBLIC RELEASE IAW AFR 190-1
ERNEST A. HAYGOOD, 1st Lt, USAF
Executive Officer, Civilian Institution Programs

17. COSATI CODES			18. SUBJECT TERMS (Continue on reverse if necessary and identify by block number)
FIELD	GROUP	SUB-GROUP	

19. ABSTRACT (Continue on reverse if necessary and identify by block number)

20. DISTRIBUTION/AVAILABILITY OF ABSTRACT ☒ UNCLASSIFIED/UNLIMITED ☐ SAME AS RPT. ☐ DTIC USERS	21. ABSTRACT SECURITY CLASSIFICATION UNCLASSIFIED
22a. NAME OF RESPONSIBLE INDIVIDUAL ERNEST A. HAYGOOD, 1st Lt, USAF	22b. TELEPHONE (Include Area Code) (513) 255-2259 22c. OFFICE SYMBOL AFIT/CI

DD Form 1473, JUN 86 *Previous editions are obsolete.* SECURITY CLASSIFICATION OF THIS PAGE

AFIT/CI "OVERPRINT"

ABSTRACT

A method has been developed to unfold photon spectra from measurements obtained with a sodium iodide counting system. A response matrix is computed by combining photon cross sections with probability distributions of path lengths for incident and internally generated photons in the energy range 0-2.8 MeV. This matrix is inverted and multiplied by a measured pulse height spectrum to obtain the photon energy distribution incident upon the detector. This deconvolution procedure provides improved information about the energy continuum of incident photons and can enhance the identification of discrete gamma energies.

Experiments were performed to verify the unfolding methodology and to evaluate the feasibility and accuracy of this technique. Measured spectra were acquired from indoor and outdoor environments and unfolded. The results show that measured spectra overestimate the number of photons below 240 keV by up to 30 %. When the total exposure was calculated directly from the measured spectra, the low energy contribution was overestimated by a factor of two. This may have implications on the interpretation and calibration of energy dependent dosimeters used for occupational and environmental monitoring.

ACKNOWLEDGEMENTS

I wish to thank my advisor and friend, Dr. Thomas B. Borak for teaching me more about radiation physics and life in general than I thought possible. His advise and guidance will stay with me throughout my career.

I am also grateful to my committee members, Drs. Shawki Ibrahim and Sanford Kern, for the time and expertise they gave towards the completion of this paper.

A word of thanks must go to my friends who I went through the program with. The good conversation, laughs, and cold beers that we all shared helped me maintain an appearance of sanity when times got rough.

Finally, my heart-felt love and gratitude go to my wife, Jenniece. Her selfless caring and understanding were the key in making my graduate studies such a success.

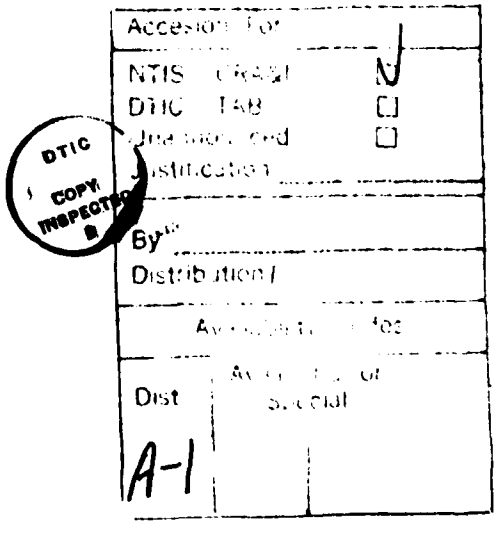

TABLE OF CONTENTS

LIST OF FIGURES

INTRODUCTION

Scintillation detectors are widely used for gamma spectra analysis and environmental radiation monitoring. However, since spectrometers only record energy deposition events within the detector, they don't necessarily show the incident photon distribution responsible for these events.

Several methods have been used to obtain this incident photon spectrum from measured pulse height distributions (Knoll 1979). Spectrum stripping can be used when partial deposition events appear exclusively below the total absorption peak. If this occurs, then the highest energy recorded must be the result of total absorption of the incident photons. Partial deposition events resulting from photons of the same energy can be subtracted from lower channels and the process repeated for the next lowest energy.

However, for many counting systems, the conditions that permit stripping are not always satisfied. Due to broad resolution, an event can be registered on both sides of the most probable channel making it difficult to determine the photon energy responsible for the observed spectra. For this situation, deconvolution or unfolding techniques must be employed.

All unfolding procedures require a set of response functions which describe partial energy deposition events in the detector for any combination of incident photons. Computing these response functions has been accomplished using Monte Carlo methods and is discussed by many authors (Hubbell 1958; Zerby 1962; Berger and Seltzer 1972). These published results are only valid for the detector and beam geometry described, so if either changes, the Monte Carlo computations must be repeated. The nature of this procedure makes it expensive and time-consuming for use in most situations.

An alternative method of computing response functions by combining photon cross sections with path length distributions was developed by Borak (1988). The only free parameters in this approach are the dimensions of the NaI(Tl) crystal and the resolution of the detection system. The feasibility of this technique was demonstrated by Merwin (1985).

Whicker (1988) continued these efforts by combining the response functions into a response matrix. The response matrix was inverted and multiplied with a pulse height spectrum to obtain the energy distribution incident upon the detector. Experiments were performed to validate the computations, and the results show the general accuracy of this technique for unfolding spectra measured with a NaI(Tl) detector.

Unfortunately, this system assumes that all photons entering the crystal had energies less than 2 MeV which does not include some high energy photons typically present in a natural radiation environment. Therefore, inherent error was introduced into this deconvolution technique when applied to measured spectra.

For example, Figure 1 shows a pulse height spectrum obtained from a residential basement and unfolded. Although ^{208}Tl was present in detectable quantities, it could not be seen in the unfolded spectrum because its photon energy, 2.61 MeV, was larger than the 2.0 MeV cutoff. Instead, it appears that the unfolding routine tried to put all the counts attributable to the high energy photons into the last channel.

The objectives of this project were to expand the response matrix calculations to 2.8 MeV and improve the unfolding process with the associated 70 X 70 response matrix.

BLANK PAGE

Figure 1. Unfolded spectrum from residential basement for photons in the energy range of 0-2 MeV incident upon a 3" by 3" NaI(Tl) detector.

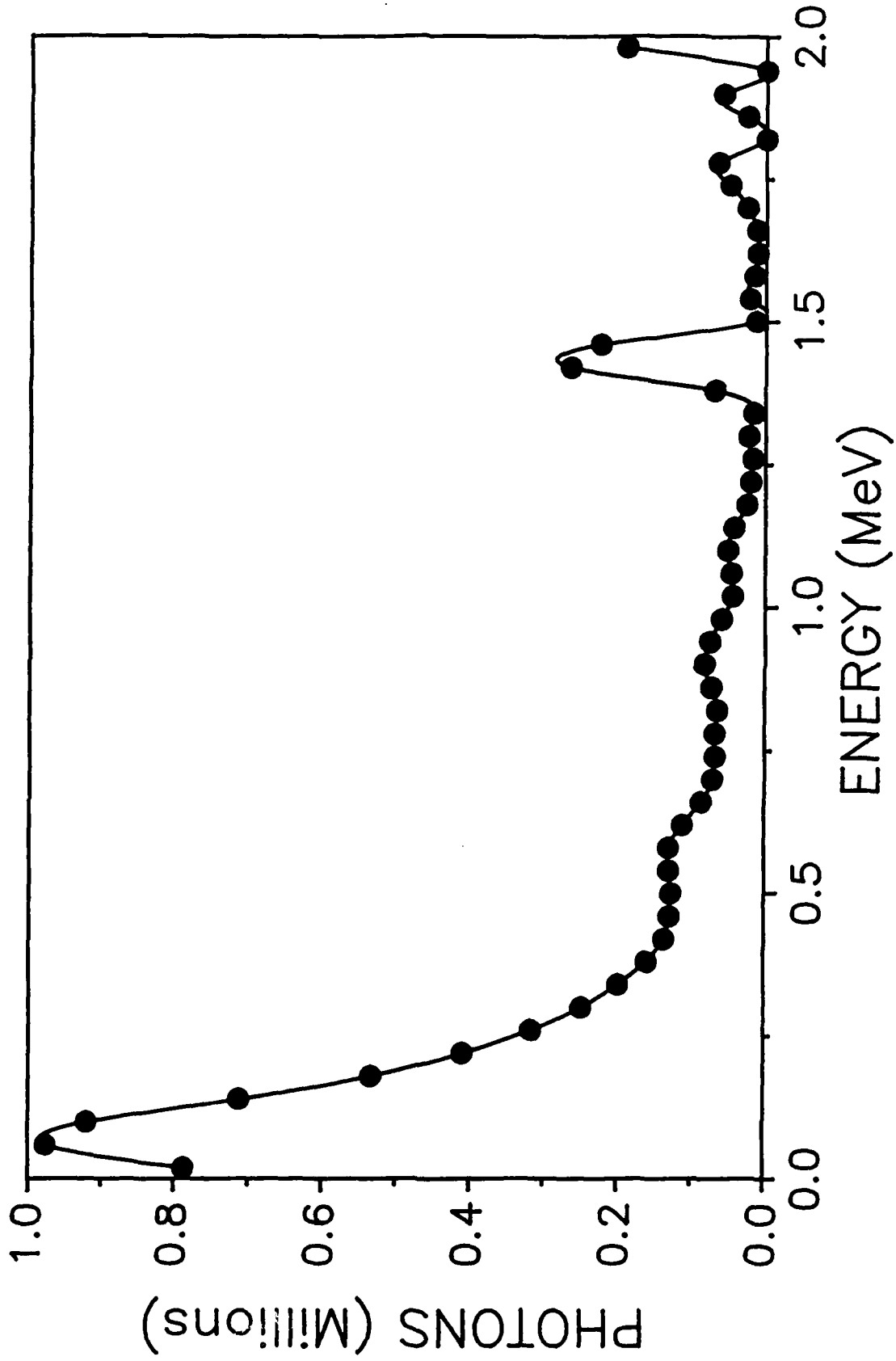
PHOTONS (Millions)
1.0
0.8
0.6
0.4
0.2
0.0
0.0
0.5
1.0
1.5
2.0
ENERGY (MeV)

METHODOLOGY

Calculation of Response Functions

To determine the response of a NaI(Tl) detector to an incident photon, the probability of interaction and the amount of energy deposited in the crystal must be computed. This was done using a computer program called COWBOY as explained in detail by Whicker (1988). A summary is included here.

The probability that an incident photon will have an initial interaction in a detector is proportional to its path length through the crystal. Since the photons can enter the detector from any angle, there are many possible path lengths. In COWBOY, the photons were assumed to be uniformly and isotropically incident (Figure 2). In geometric probability, this assumption is referred to as μ-randomness, and the resulting path lengths will have a defined probability distribution.

A similar assumption was made for the internally generated photons (Figure 3). These photons result from incoherent scattering and pair production interactions within the NaI(Tl) crystal. Although secondary photons have a preferential scattering angle with respect to the primary photon, the direction in the coordinate frame of the detector

Figure 2. Schematic representation of uniformly and isotropically incident photons upon a cylindrical detector.

External Path Length Distribution

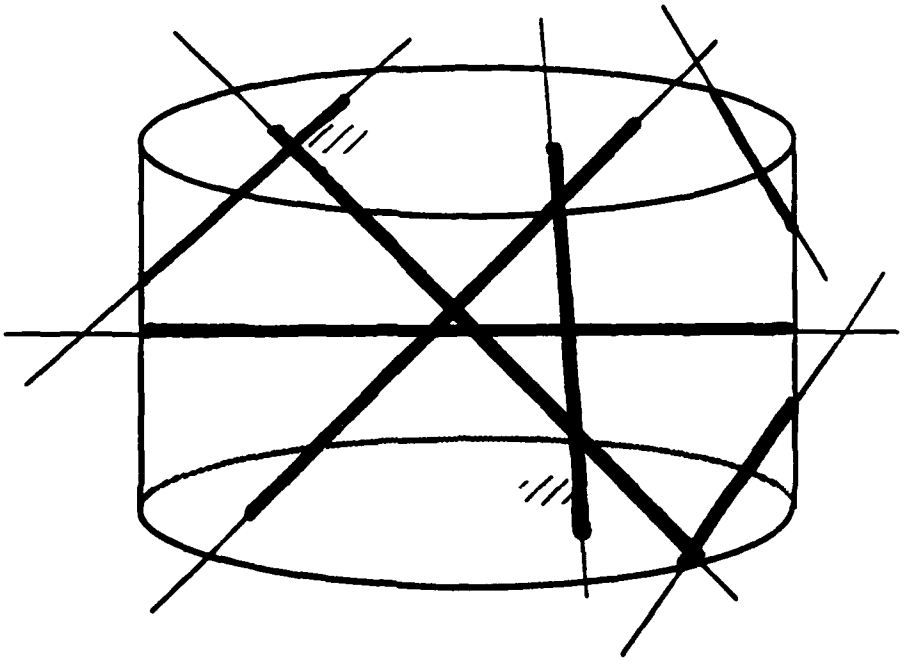

μ Randomness

Figure 3. Schematic representation of uniform and isotropic secondary photons generated in a cylindrical detector.

Internal Path Length Distribution

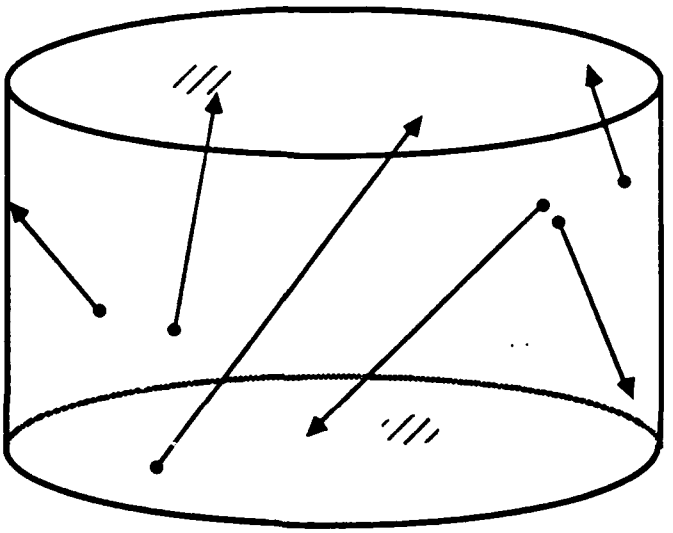

I Randomness

is random since the primary photon was incident randomly. In geometric probability, this is described as I-randomness, and the path lengths can also be characterized by a defined probability density function.

For a cylindrical crystal with a diameter equal to its height (elongation = 1), the path length distributions are shown in Figure 4. These probability density functions were generated using a simple Monte Carlo code (Borak 1988) and are incorporated into COWBOY. Since the internal path length distribution is computed from the external distribution, the Monte Carlo process is used only once for a specified detector geometry. If a different elongation is used, COWBOY only requires the new path length distributions.

The probability that a photon will interact when passing through a crystal is dependent on these path length distributions and the total attenuation coefficient, μ. In COWBOY, μ is calculated using the photoelectric, Compton, and pair production cross sections. Equations to describe these energy dependent parameters were obtained by fitting polynomial functions to tabulated data. The photoelectric cross sections were determined from Grodstein (1957); Compton cross sections were found in Hubbell *et al.* (1975); and pair production cross sections were obtained from Hubbell *et al.* (1980).

Figure 4. External and internal path length probability density functions for a right circular cylinder with an elongation = 1 (3" X 3").

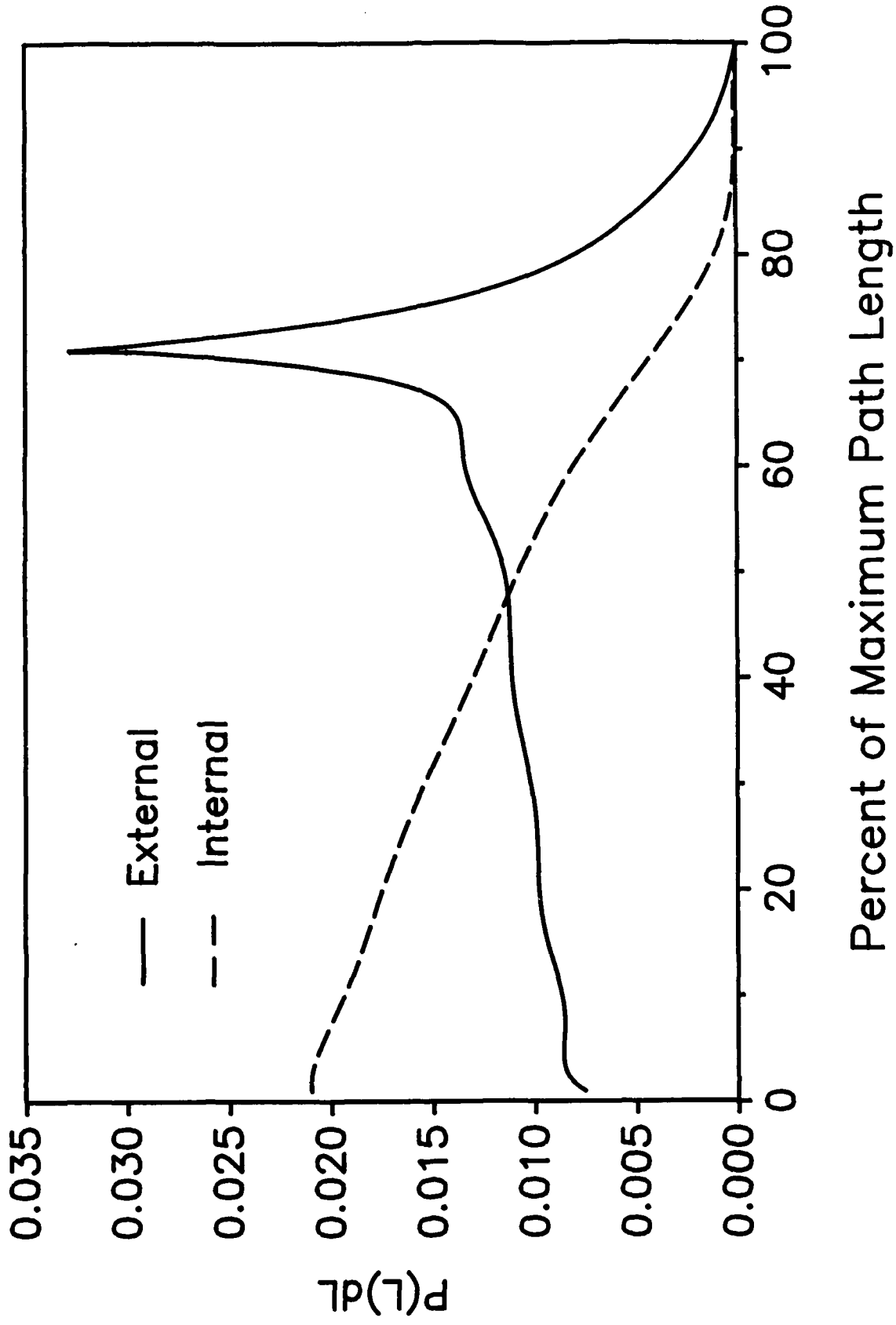
P(L)dL
0.035
0.030
0.025
0.020
0.015
0.010
0.005
0.000
0
20
40
60
80
100
Percent of Maximum Path Length
External
Internal

In determining the probability of interaction, the photoelectric, Compton and pair production phenomena were combined into the total attenuation coefficient. However when considering energy deposition in the crystal, these events must be examined separately. For photoelectric interactions, all of the photon energy was assumed to be deposited in the crystal. For Compton scattering, the Klein-Nishina formula was used to determine the probability for obtaining a recoil electron. Total deposition was then assumed for each recoil electron. For pair production, total absorption of the positron and electron was assumed. The annihilation photons were allowed to undergo one interaction, depositing their energy accordingly.

Therefore, the probability for an energy deposition event from an incident photon is based on the sum of three independent events, each of which is represented by a corresponding probability distribution. COWBOY treats the internally generated photons in a similar manner. For this project, all source photons were allowed to interact a maximum of four times. A scattered photon that had not been totally absorbed after the fourth collision was assumed to escape the crystal.

The final step in the calculation is to assign the energy deposition probabilities to the appropriate channels incorporating the resolution of the detection system.

To determine the accuracy of this methodology, a response function was computed for monoenergetic photons at 662 keV and compared with a measured pulse height distribution for ^{137}Cs.

Expansion of COWBOY

After the generation of the response functions was verified, the program was expanded to include photon energies up to 2.8 MeV. The time required to execute the enlarged version of the program made it impractical to use on a microcomputer. Therefore, the program was downloaded, compiled, and run on a CYBER 205 supercomputer.

Expanding the program involved revising the subroutines used to compute the Compton and pair production cross-sections. Since the existing functions were only valid to 2.0 MeV, new functions were obtained by fitting the tabulated data out to 5.0 MeV using regression techniques. These new parameters were incorporated into COWBOY, and the dimensions of arrays and executions statements were increased.

Before downloading the revised program to the mainframe, a test was run to compare the two versions. A response function was generated for eight sets of monoenergetic photons equally spaced in energy from 0-2 MeV. The output from the expanded program was compared with the previous version to ensure that the same results were obtained.

After transferring the program to the CYBER, a similar verification test was performed to ensure no errors were accidentally introduced during downloading and debugging.

Unfolding Methodology

The CYBER 205 supercomputer was used to generate the complete response matrix, R, by combining the individual response functions. The energy range from 0 to 2.8 MeV was divided up into 40 keV intervals which yielded a 70 X 70 matrix. The elements of the matrix, R_{ij}, correspond to the probability that an incident photon of energy j, deposits energy in channel i. Thus, the number of counts in a channel, N_i, can be expressed as (Knoll 1979):

$$N_i = R_{ij} * S_j$$

where S_j is the number of incident photons with energy j.

By inverting the response matrix, it is possible to unfold the photon energy distribution from the measured data:

$$S_j = R_{ij}^{-1} * N_i$$

Matrix inversion was performed with the program INVERT by standard Gauss-Jordan elimination method (Bevington 1969). The program UNFOLD multiplied the inverted matrix with the pulse height distribution to obtain the source spectrum. In spite of the increased dimensions of the response matrix, the matrix inversion and multiplication were accomplished on an IBM compatible 286 AT microcomputer in less than 1 minute.

Verification Using Computed Spectra

To test the deconvolution technique, response functions were computed for 100 incident photons at different energies and unfolded. The unfolded spectra were analyzed to ensure that the expected source spectrum was produced.

Deconvolution of Measured Spectra

The unfolding methodology was applied to measured pulse height distributions from four different environments. The results from each location were compared to evaluate the differences between measured and unfolded spectra especially at low energies. Using the mass absorption coefficients for air, the exposure rate from both the measured and unfolded data were computed. These values were compared to determine the contribution to exposure from low energy photons.

Filtering Routine

A pattern of channel-to-channel oscillations which become undamped at high energies was seen in the unfolded spectrum (Whicker 1988). Different digital filtering techniques were used to eliminate these artifacts while still preserving the incident spectra. Because the oscillations were almost symmetric and had a period of two channels, a series of three point smooths were used on the data.

For this project, all unfolded spectra were filtered using the same technique. One 3-point smooth was applied to the measured (or computed) pulse height distribution. After unfolding, three successive 3-point smooths were used. Finally, just before saving the unfolded spectrum, all channels with a negative number of photons were set to zero.

Detector Efficiency

As a final test of the system, the efficiency (or yield) of the 3" X 3" NaI(Tl) detector was computed as a function of photon energy. The response functions created with COWBOY take into consideration photons which pass through the detector without depositing any energy. Therefore, the area under a pulse height distribution computed for a 100 incident photons represents the percent efficiency of the counting system. This efficiency was computed for every 40 keV interval from 0-2.8 MeV and compared with published values (Harshaw 1975).

RESULTS AND DISCUSSION

Calculation of Response Functions

To determine the accuracy of the response functions generated by COWBOY, a pulse height distribution was computed for 662 keV photons and compared to a ^{137}Cs spectra that was measured. The computed and measured data were normalized to the maximum value found in their respective distributions.

As shown in Figure 5, the total absorption peaks show excellent agreement. The measured spectrum shows a backscatter peak and also has a higher Compton plateau because source photons were scattered before entering the crystal.

Whicker (1988) performed analogous verification studies using computed response functions and published spectra for ^{137}Cs, ^{60}Co, and ^{22}Na and obtained similar results.

Expansion of COWBOY

The polynomial equations for Compton and pair production cross sections as a function of photon energy are listed in the appendix. The coefficients were obtained using regression techniques, and they predict the tabulated data within one percent (Figures 6 and 7).

Figure 5. Comparison between a measured ^{137}Cs spectrum and a computed response function for 662 keV photons incident upon a 3" X 3" NaI(Tl) crystal. The distributions were normalized to the maximum value in each spectrum.

NORMALIZED RESPONSE
1.0
0.8
0.6
0.4
0.2
0.0
0.0
0.2
0.4
0.6
0.8
1.0
ENERGY (MeV)
Computed Response Function
Measured Spectrum

Figure 6. Published Compton cross sections (Hubbell *et al.* 1975) and the predicted values used for computing the response functions.

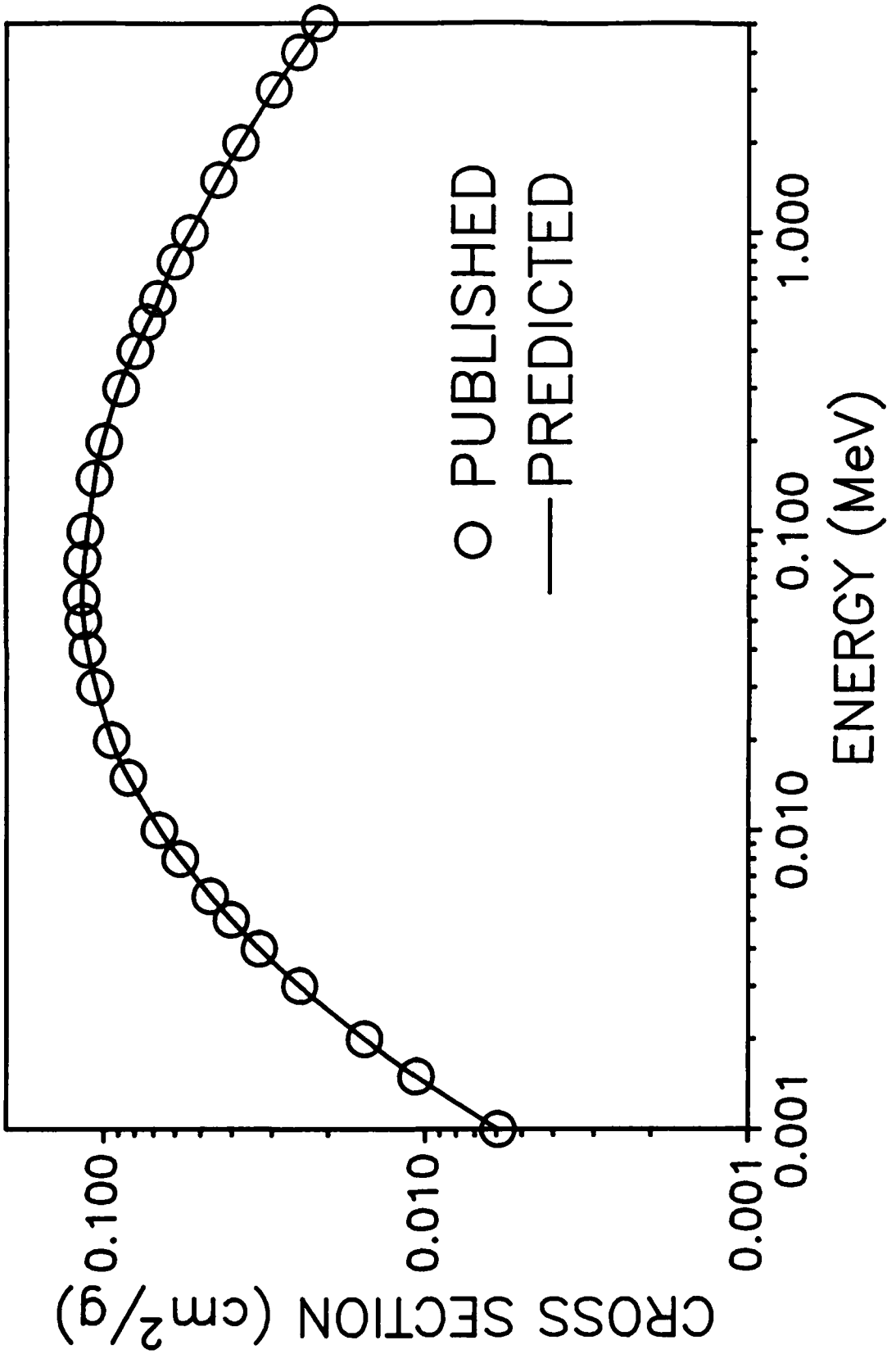
CROSS SECTION (cm²/g)
0.100
0.010
0.001
0.001
0.010
0.100
1.000
ENERGY (MeV)
O PUBLISHED
— PREDICTED

Figure 7. Published pair production cross sections (Hubbell *et al.* 1980) and the predicted values used for computing the response functions.

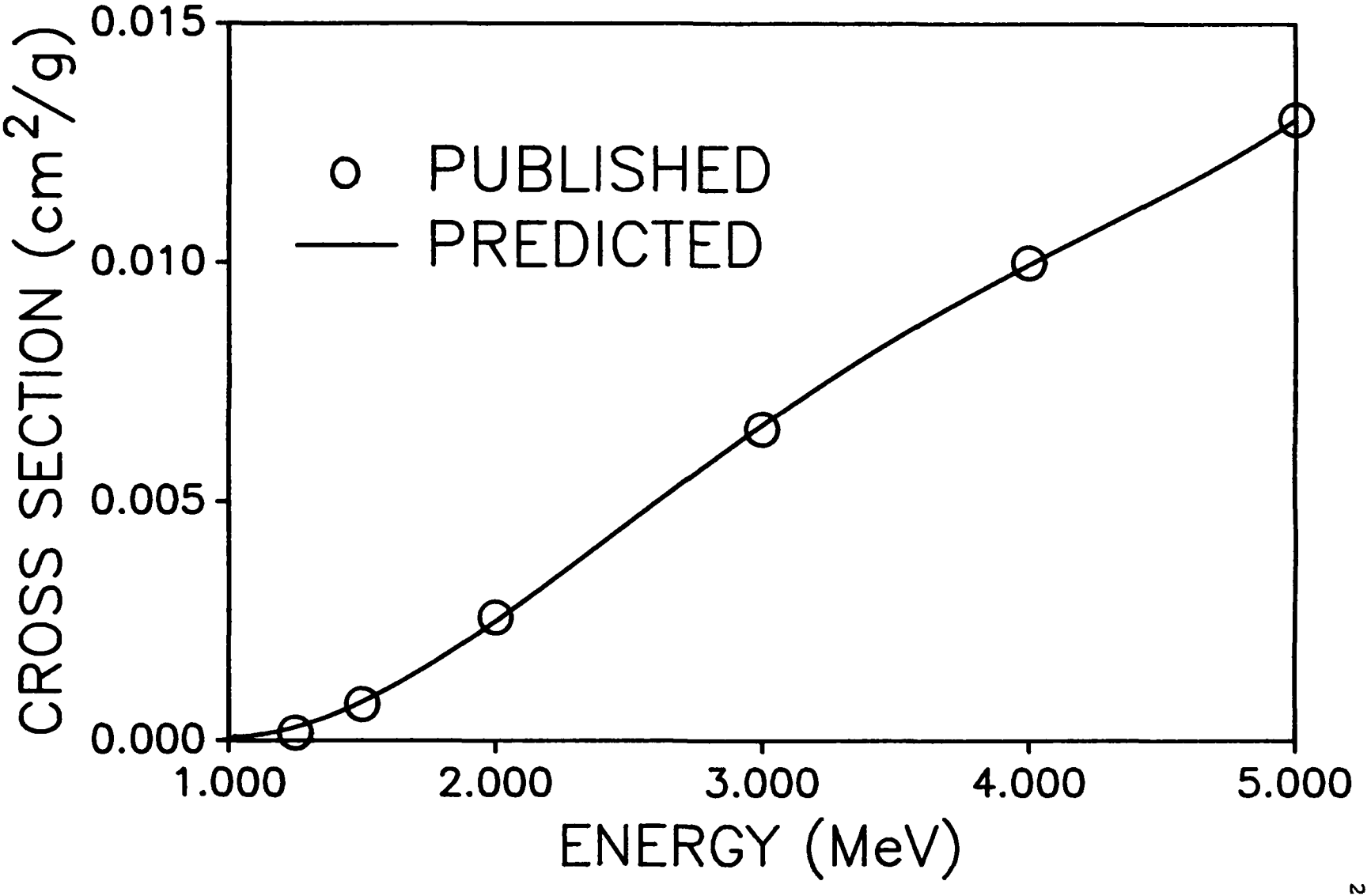
0.015
0.010
0.005
0.000
CROSS SECTION (cm²/g)
PUBLISHED
PREDICTED
1.000
2.000
3.000
4.000
5.000
ENERGY (MeV)

n expanding the program to 2.8 MeV, it was not necessary to revise the photoelectric cross sections because this effect is negligible above 2.0 MeV. Therefore, the values in Whicker (1988) were used.

To ensure that the expansion of COWBOY and the revision of the cross section subroutines did not alter the response function calculations, the outputs from both program versions were compared. Using identical inputs, a complicated response function covering the energy range 0-2 MeV was generated with both programs. The two pulse height distributions agreed within 0.05 % as shown qualitatively in Figure 8.

Following this test, the program was transferred to the CYBER 205 supercomputer. Instructions for downloading, compiling, and running the program on the mainframe are included in a separate report (Wannigman 1989).

Before generating the complete response matrix, one final verification was performed. A response function for 100 photons incident at 2.79 MeV was created using both the microcomputer and the CYBER. Because it took the PC over six hours to compute a four interaction pulse height spectrum for photons at this energy, the incident photons were only allowed to undergo two collisions. This reduced the computing time on the IBM compatible to about 20 minutes. The output from both hardware devices were identical (Figure 9).

Figure 8. Comparison of response functions generated using both the revised version of COWBOY and the previous version (Whicker 1988) for eight sets of monoenergetic photons allowed to undergo four interactions in a 3" by 3" NaI(Tl) crystal.

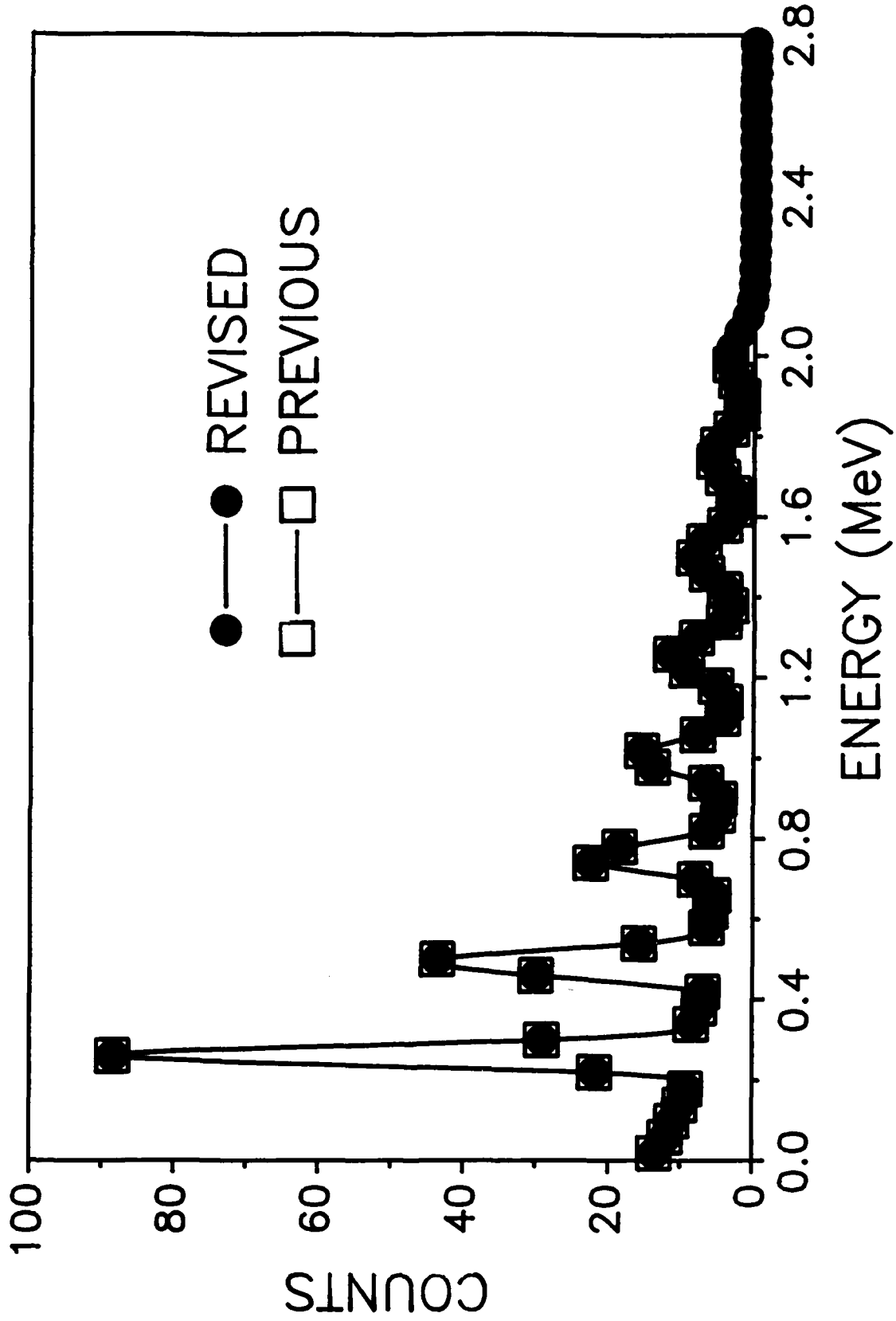
REVISED
PREVIOUS
COUNTS
ENERGY (MeV)
0
20
40
60
80
100
0.0
0.4
0.8
1.2
1.6
2.0
2.4
2.8

Figure 9. Comparison of response functions generated using both hardware devices used to run COWBOY for 100 2.79 MeV photons allowed to undergo two collisions in a 3" X 3" NaI(Tl) crystal.

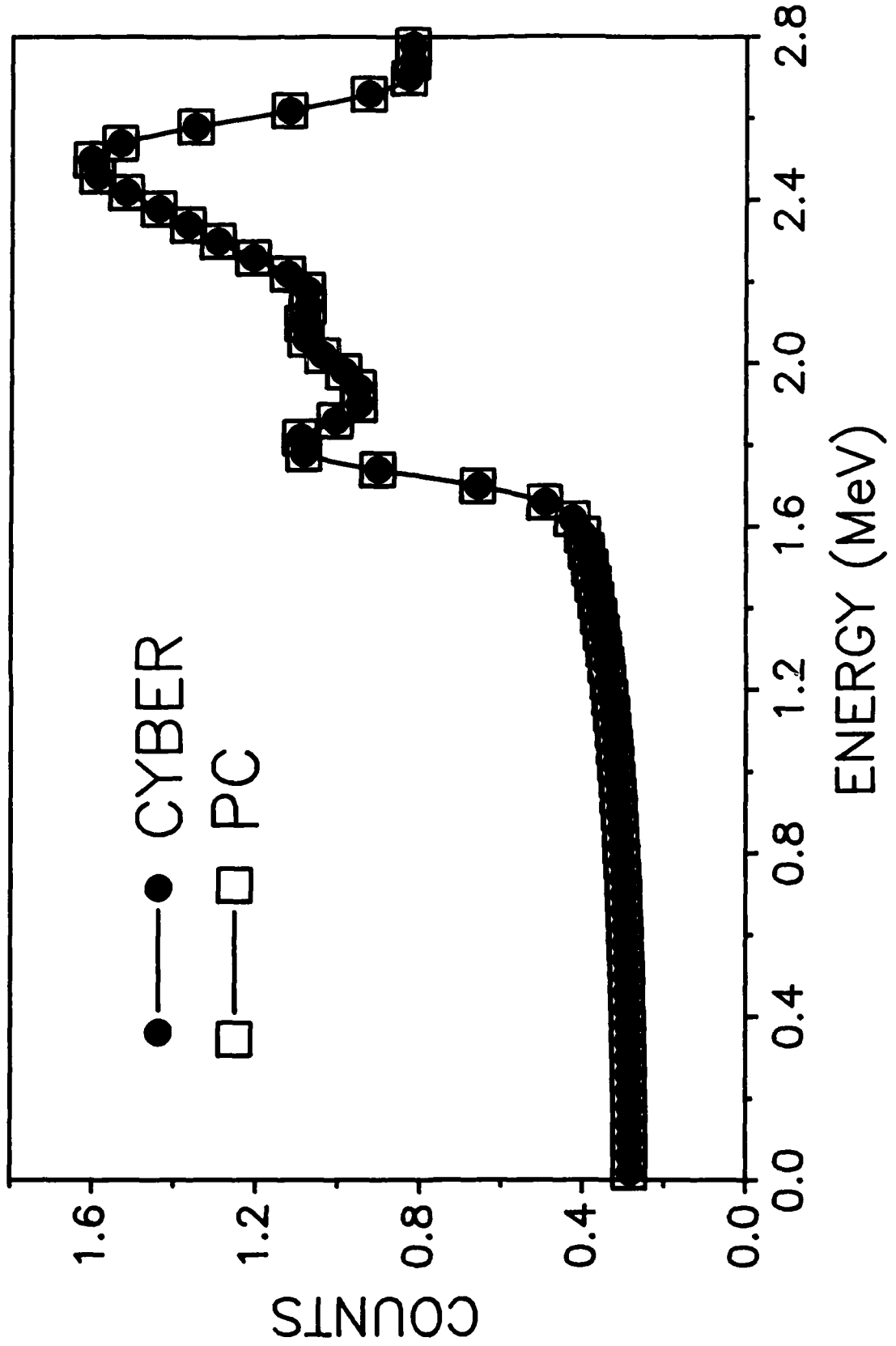
CYBER
PC
COUNTS
ENERGY (MeV)
0.0
0.4
0.8
1.2
1.6
2.0
2.4
2.8

Verification Using Computed Spectra

A response function was generated for three sets of monoenergetic photons, 100 photons each, at energies of 1.0, 1.8, and 2.6 MeV. Unfolding this pulse height distribution produced exactly 100 photons at each of the incident energies (Figure 10). The unfolding was exact because each of the incident energies corresponded to the center of one of the 40 keV intervals and was identical to the energy used in generating the response function for that interval.

Next, a response function was computed for energies that were not in the center of an interval (Figure 11). When this spectra was unfolded, the photons were not confined to a single channel. Instead, they were expressed as a broad peak centered around the energy of the incident photons. Numerical integration showed that the areas under each peak were all within 2 % of the 100 photons, so the unfolding process still produced the expected source spectrum.

Since the deconvolution methodology was shown to accurately unfold computed spectra, it was applied to measured pulse height distributions from four different environments.

Deconvolution of Measured Spectra

The photon spectra in a residential basement was measured with a 3" X 3" NaI(Tl) detector and unfolded (Figure 12). The measured pulse height distribution is higher than the incident photon distribution below 240 keV. The reverse is true above

Figure 10. Computed response function and unfolded energy distribution for three sets of photons incident with energies in the center of a 40 keV interval.

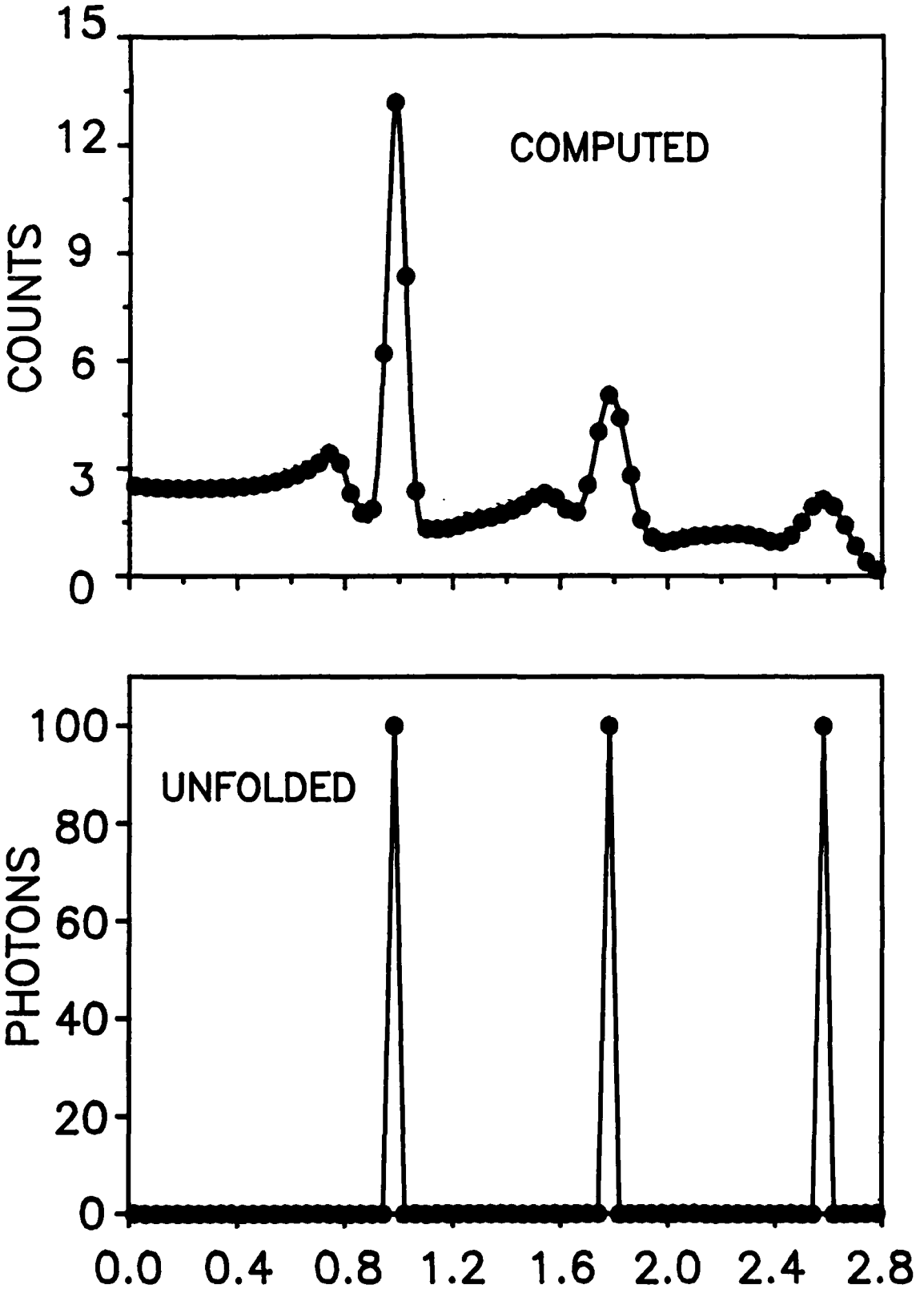
15
12
9
6
3
0
COUNTS
COMPUTED
100
80
60
40
20
0
PHOTONS
UNFOLDED
0.0
0.4
0.8
1.2
1.6
2.0
2.4
2.8

Figure 11. Computed response function and unfolded energy distribution for six sets of photons incident with energies not in the center of an interval.

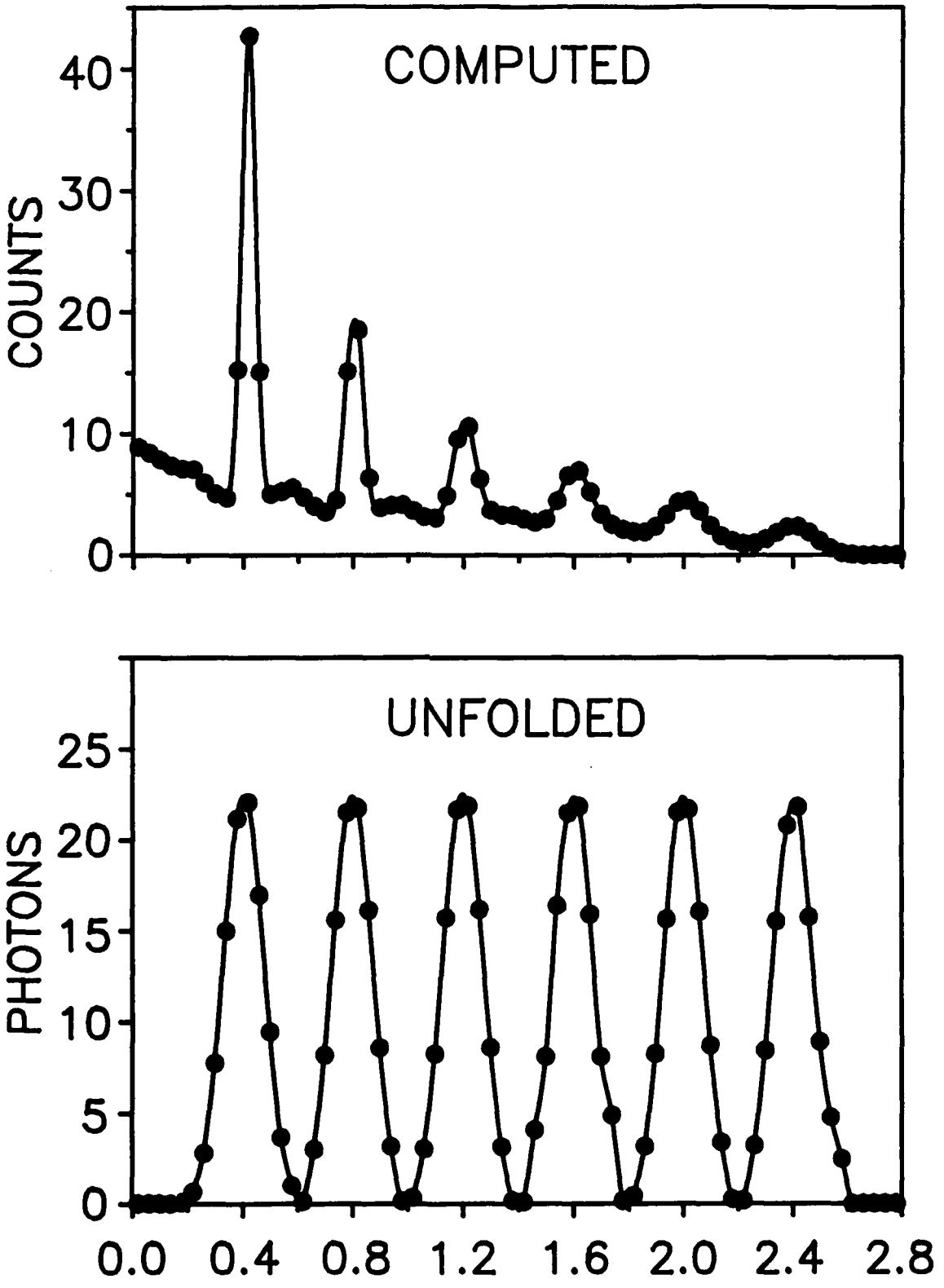
COMPUTED
COUNTS
40
30
20
10
0
UNFOLDED
PHOTONS
25
20
15
10
5
0
0.0
0.4
0.8
1.2
1.6
2.0
2.4
2.8

Figure 12. Measured spectra from a residential basement and the unfolded photon distribution incident upon a 3" by 3" NaI(Tl) crystal.

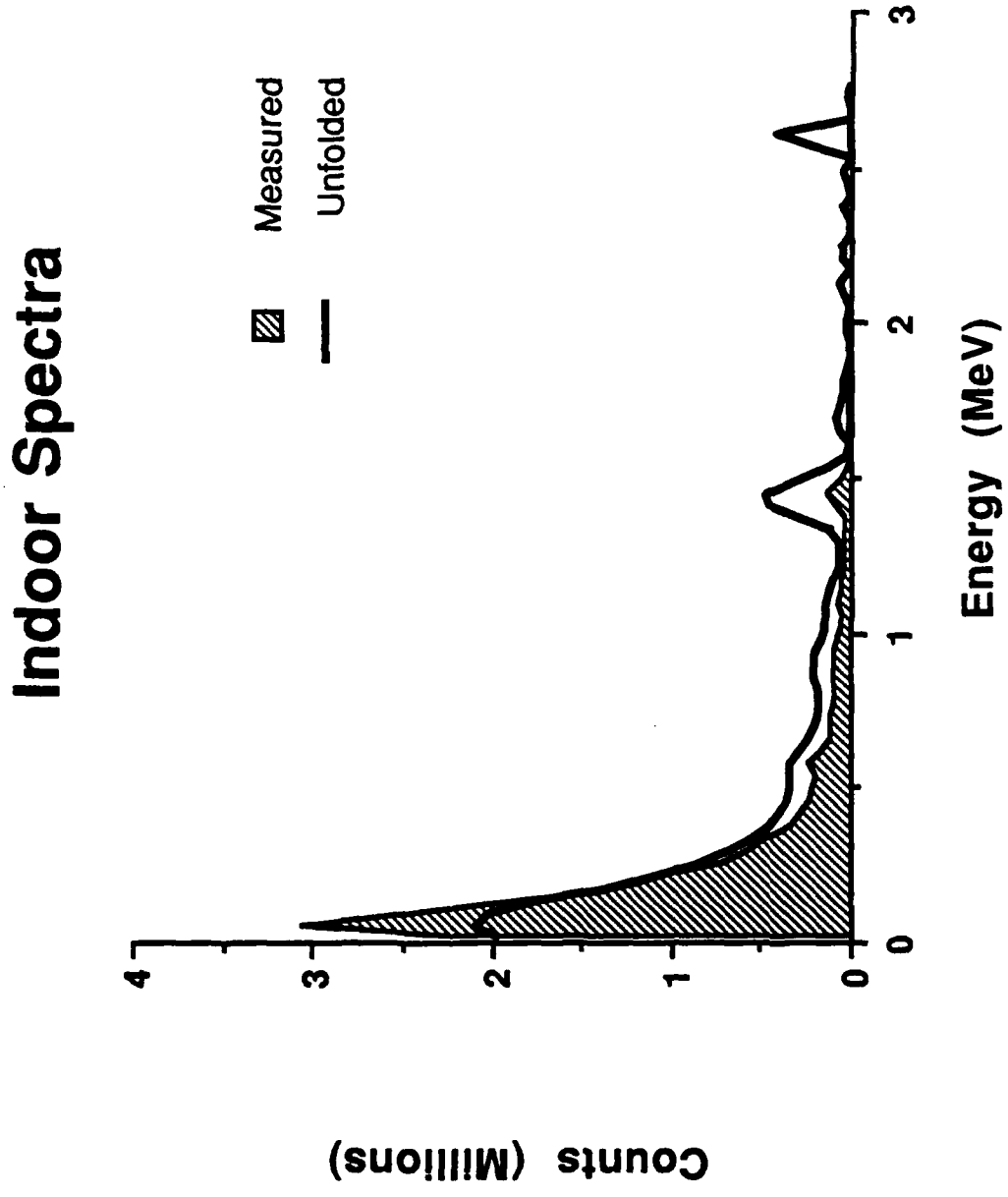
Indoor Spectra
Measured
Unfolded
Counts (Millions)
Energy (MeV)
0
1
2
3
4

240 keV because the unfolding process reassigns partial energy deposition events to the appropriate photon energy. The total area under the unfolded spectrum is larger than the measured spectrum because the unfolding also accounts for photons which pass through the detector without depositing any energy. Although more validation is required before a detailed interpretation of the unfolded spectrum can be made, it is clear that the deconvolution amplifies discrete gamma energies such as the peaks for ^{40}K (at 1.46 MeV) and ^{208}Tl (at 2.61 MeV).

Similar results were obtained from an outdoor environment (Figure 13). Again, the unfolding process identifies counts associated with partial deposition events and assigns them to the channel corresponding to the energy of the incident photon.

A pulse height distribution was also measured at different distances from a storage cabinet containing various calibration sources. The spectra near the source cabinet (Figure 14) were dominated by soft photons from scattered radiation, and this low energy portion completely overpowers the structure at higher energies. Away from the source cabinet, the flux of these soft photons was reduced, and the peaks from each source could be seen (Figure 15).

An estimate of the exposure in the different environments was found by multiplying the photon energy distributions by the mass absorption coefficients for air. The relative contribution from photons below 240 keV was computed for both

Figure 13. Measured spectra from an outdoor environment and the unfolded photon distribution incident upon a 3" by 3" NaI(Tl) crystal.

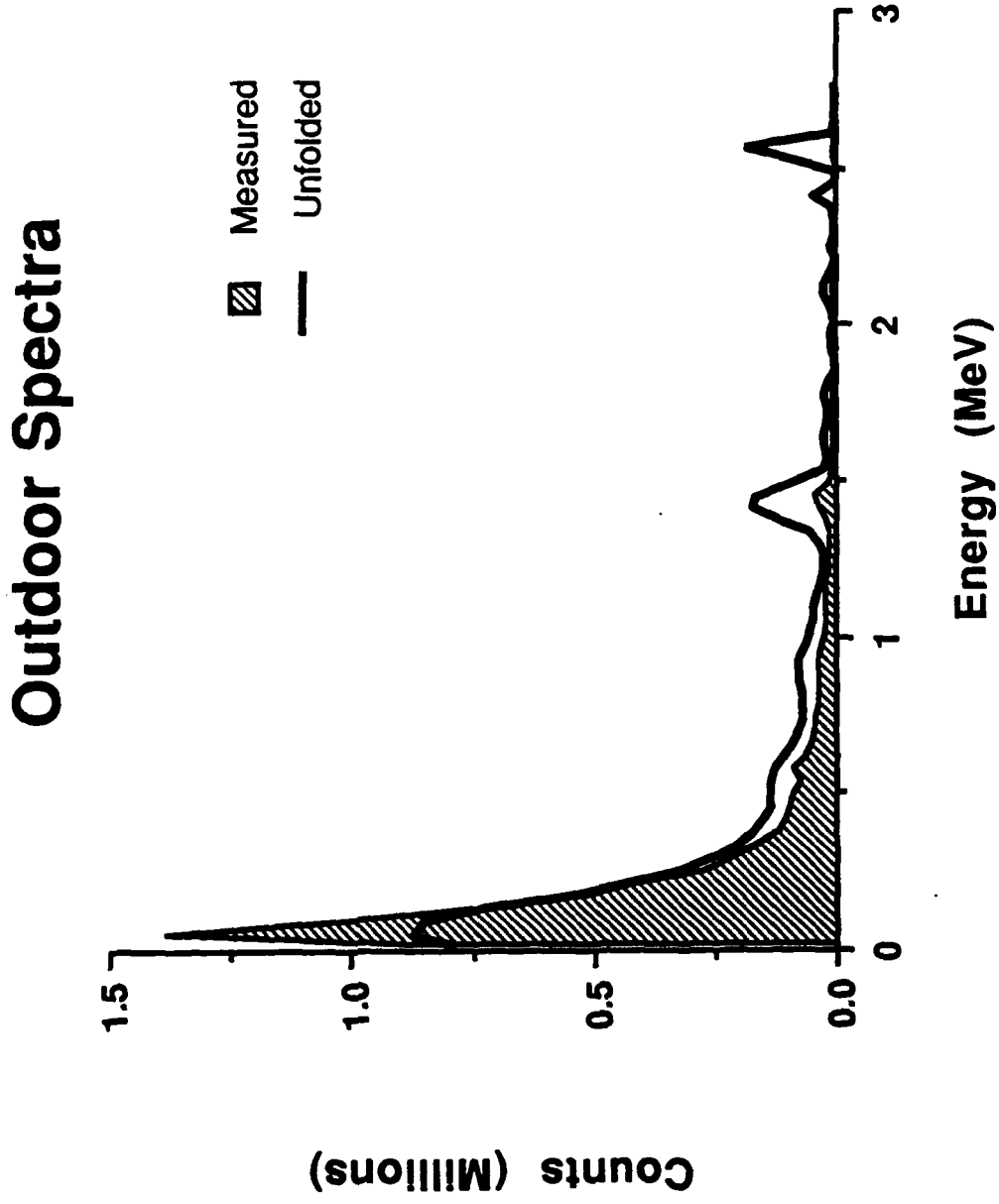
Outdoor Spectra
Measured
Unfolded
Counts (Millions)
1.5
1.0
0.5
0.0
0
1
2
3
Energy (MeV)

Figure 14. Measured spectra near a source storage cabinet and the unfolded photon distribution incident upon a 3" by 3" NaI(Tl) crystal.

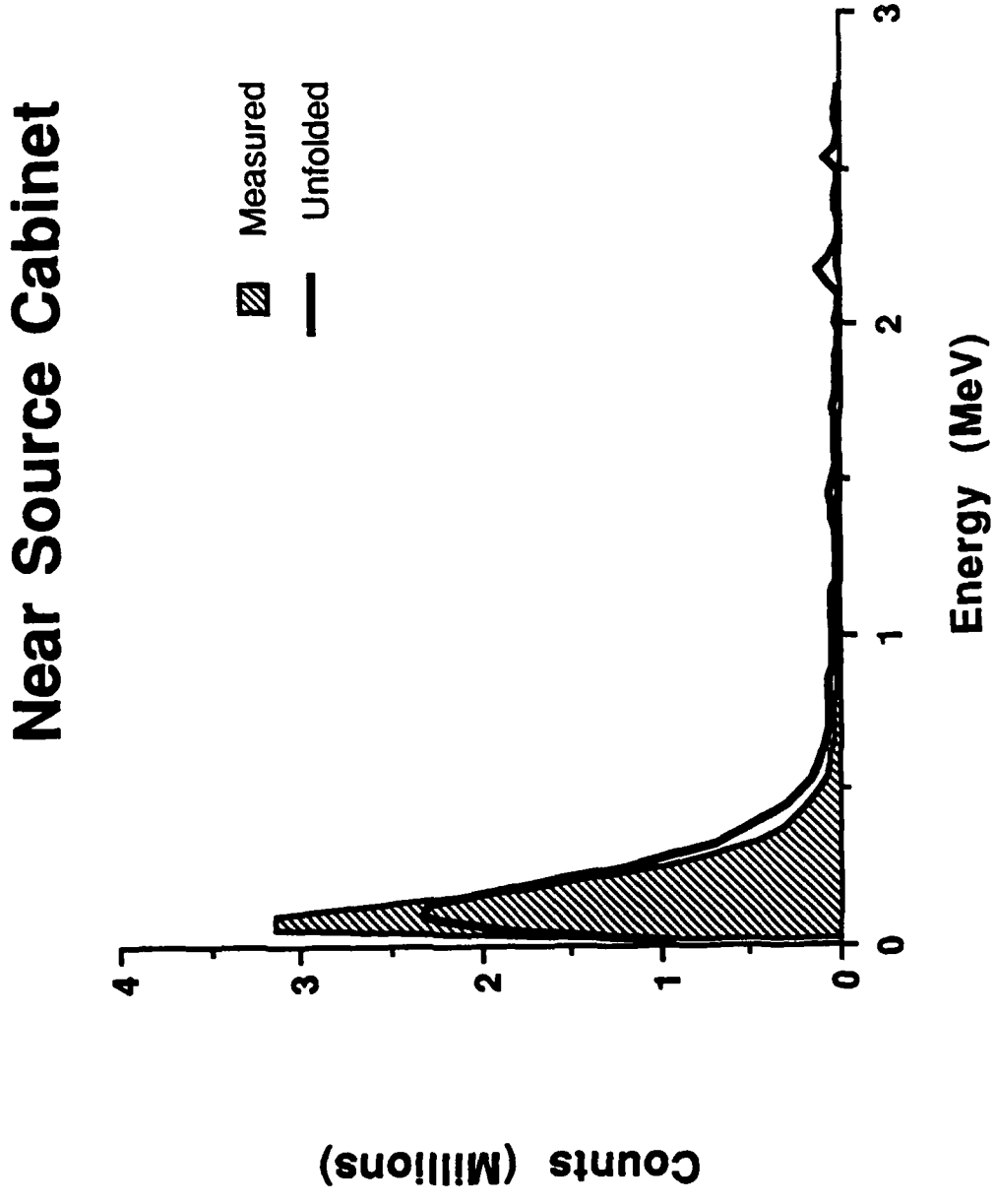
Near Source Cabinet
Measured
Unfolded
Counts (Millions)
Energy (MeV)
0
1
2
3
4

Figure 15. Measured spectra away from a source storage cabinet and the unfolded photon distribution incident upon a 3" by 3" NaI(Tl) crystal.

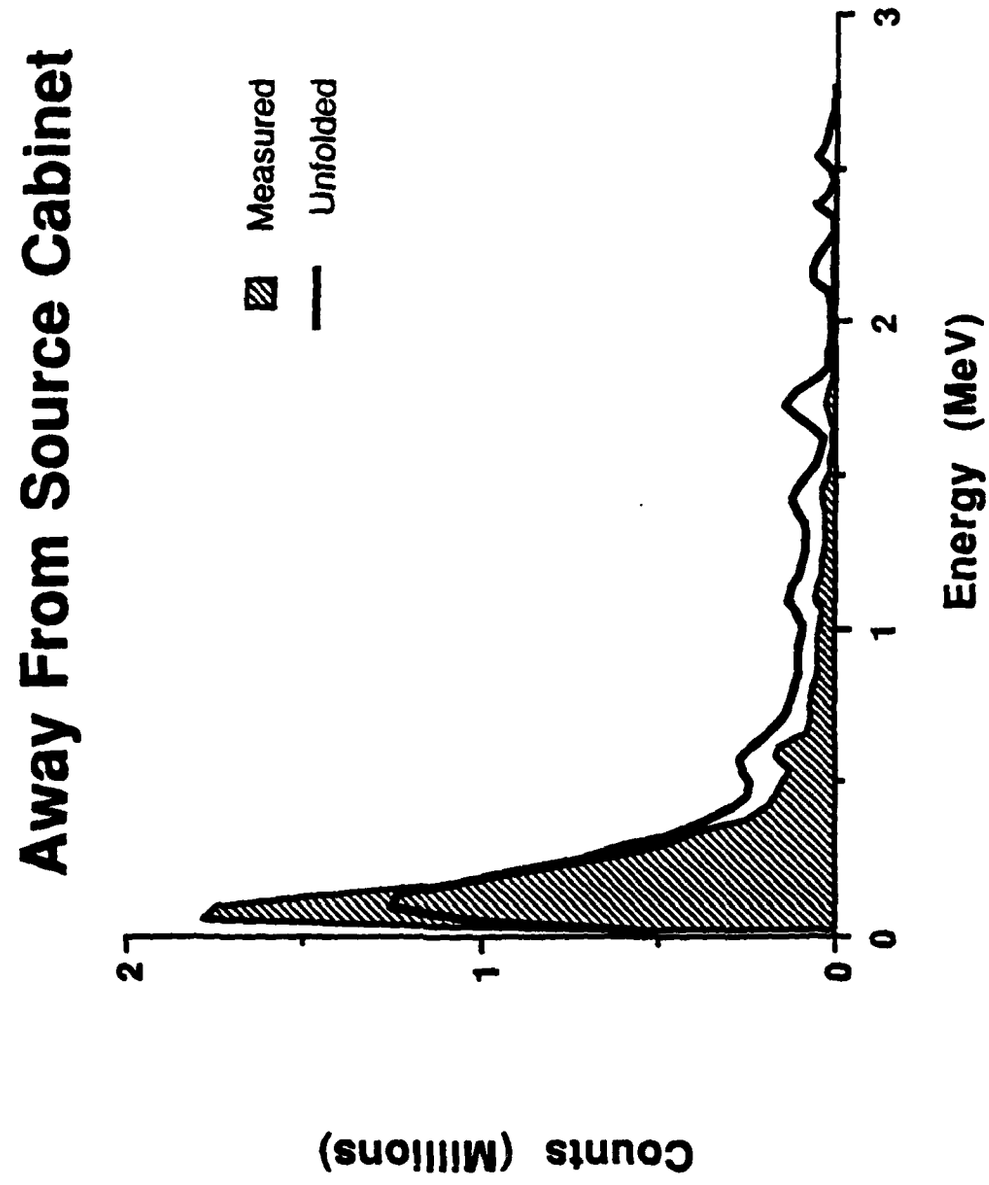
Away From Source Cabinet
Measured
Unfolded
Counts (Millions)
Energy (MeV)
0
1
2
3
0
1
2

the measured and unfolded spectra. As shown in Table 1, the incident photon distribution was significantly different from the measured spectra at these low energies.

Table 1. Relative contributions of low energy photons (below 240 keV) to the pulse height distribution and exposure rate computation.

	No. of photons		Exposure rate	
Location	Measured	Unfolded	Measured	Unfolded
Indoor	68 %	53 %	34 %	17 %
Outdoor	71	56	36	19
Near source cabinet	78	67	49	31
Away from cabinet	65	49	29	14

For example, the measurements from the indoor environment indicate that nearly seventy percent of all energy deposition events were below 240 keV. However, only 53 % of the photons in the unfolded spectra had these energies -- a difference of nearly 30 %.

Similar results were obtained when comparing the exposure rate estimations. If used directly, the low energy counts in the measured spectra would estimate that 34 % of the total exposure is in this region. After unfolding, this drops to 17 %.

This observation was seen in each of the other environments. The measured spectra consistently overestimated the low energy component by 25 to 30 percent. If used directly, this would provide a two-fold overestimation of the soft photon contribution to exposure.

Detector Efficiency

As used here, the efficiency of the 3" X 3" NaI(Tl) detector refers to the percent of all the photons that pass through the detector which deposit a least some energy. It is related to the photon cross sections and is therefore a function of the gamma energy.

The efficiency was computed by using COWBOY to generate a separate response function for every 40 keV interval from 0 to 2.8 MeV, and then numerically integrating the area under each pulse height distribution. The published efficiencies were taken from an equipment brochure (Harshaw 1975) for a point source located on the surface of the detector. Because only 50 % of the point source photons have an opportunity to enter the crystal, the published values were doubled before being compared with the predicted values.

As shown in Figure 16, the program accurately computes the energy dependent efficiencies for the specified detector geometry.

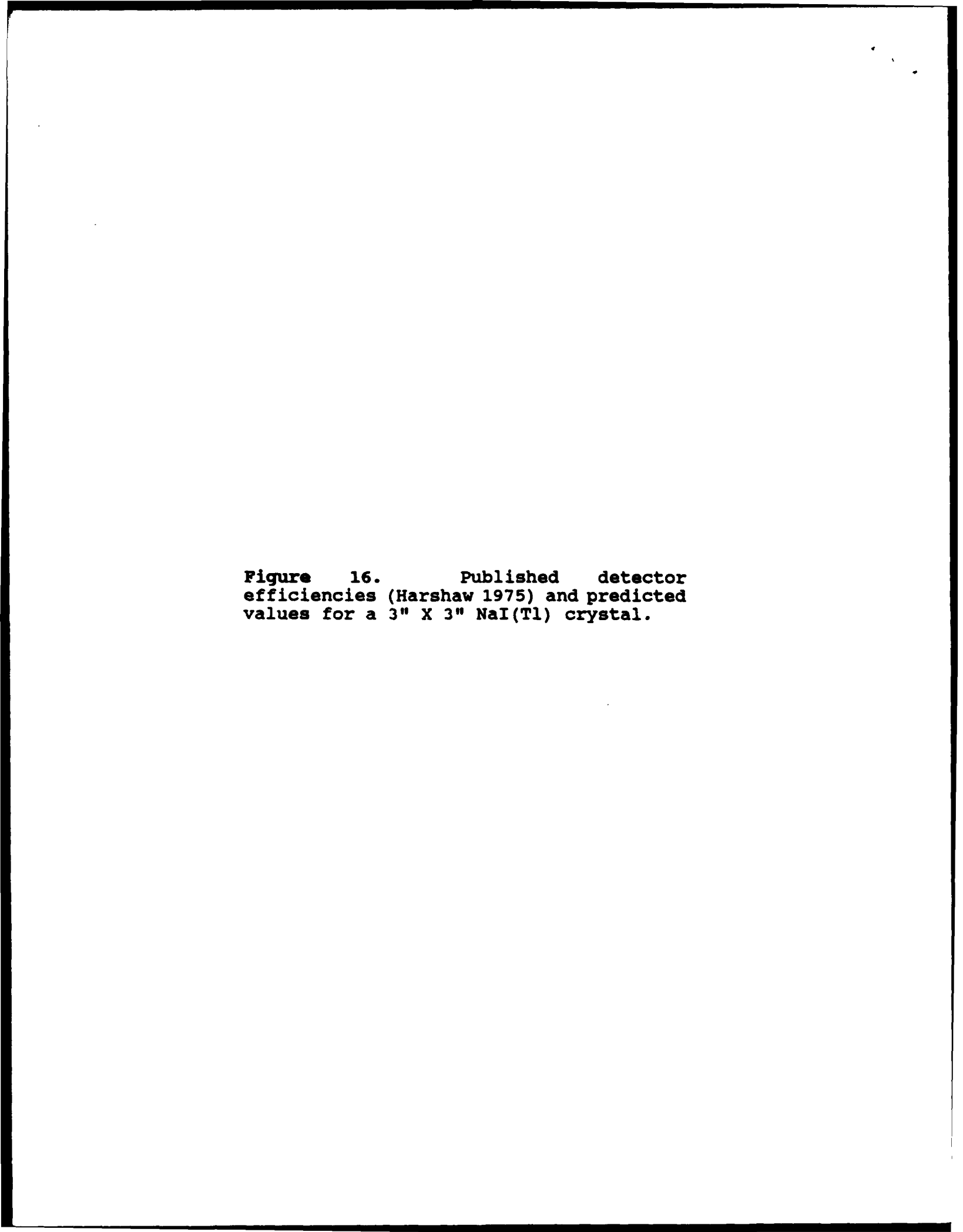

Figure 16. Published detector efficiencies (Harshaw 1975) and predicted values for a 3" X 3" NaI(Tl) crystal.

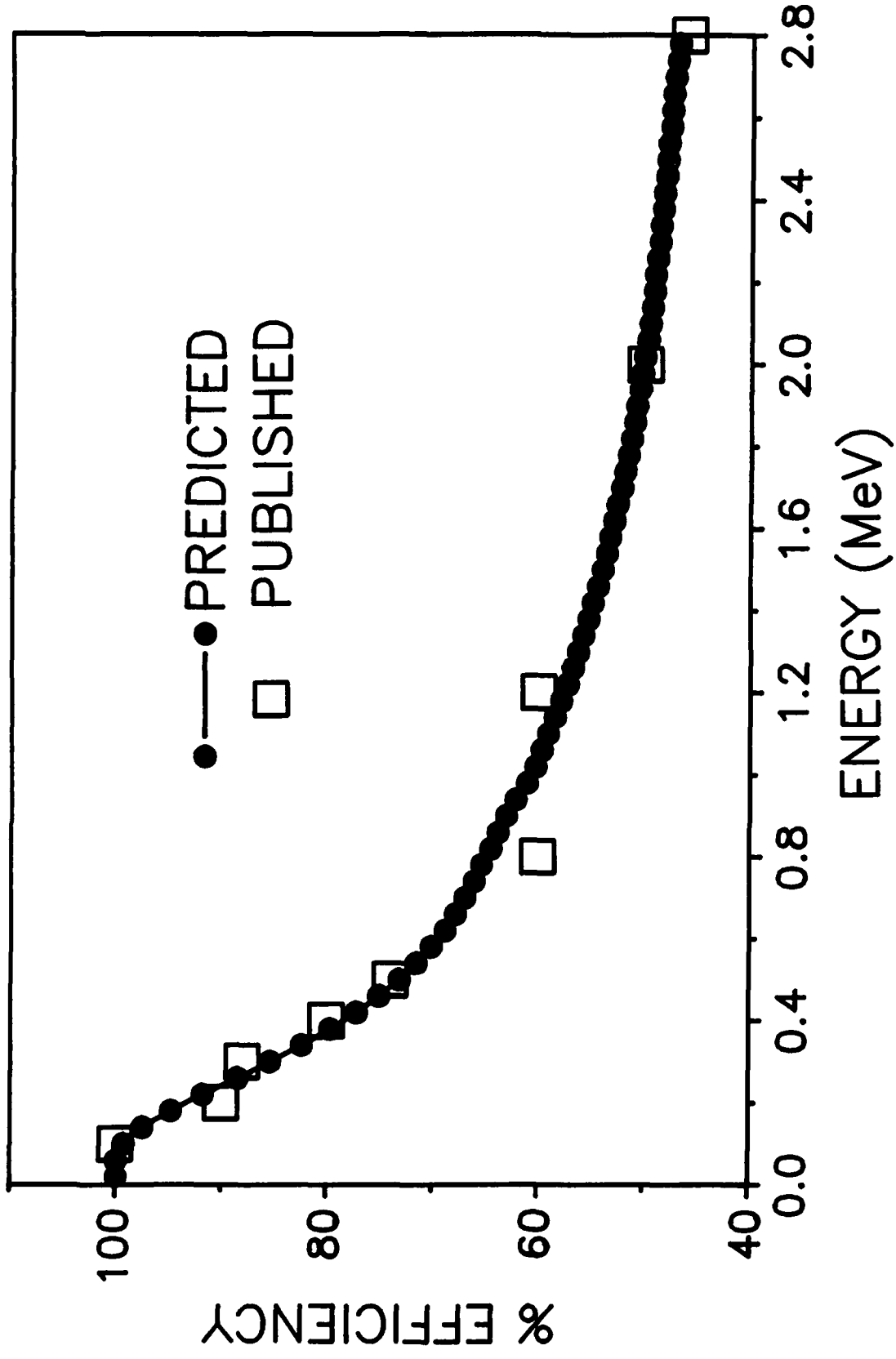
% EFFICIENCY
100
80
60
40
0.0
0.4
0.8
1.2
1.6
2.0
2.4
2.8
ENERGY (MeV)
PREDICTED
PUBLISHED

CONCLUSIONS

A method has been developed to unfold environmental photon energy distributions from measured spectra. Response functions were computed using path length probability distributions and photon cross sections. Using matrix inversion, the incident photon spectra was unfolded from pulse height measurements in different environments. Verification studies were performed to indicate the feasibility and general accuracy of this deconvolution methodology for spectra obtained with a NaI(Tl) counting system.

The results showed that there are dramatic differences between measured and unfolded spectra especially below 240 keV, and although this isn't high resolution spectroscopy, the unfolding process enhanced peaks that could not be seen in the measurements. The deconvolution also demonstrated how partial energy deposition events could lead to an overestimation of exposure. This, in turn, can have important implications on the interpretation and calibration of energy dependent instruments used for occupational and environmental monitoring.

Further testing of the unfolding methodology used in this project is needed, and there are several possible areas to address in future research. The most important of these is the need to reduce the time required for computing the

response functions. The most time consuming part in running COWBOY is combining the probabilities of energy deposition from multiple events within the detector. This is based on the convolution theorem for the sum of random variables. The computational effort might be reduced considerably by using fast Fourier transformations.

Validation studies need to be conducted using a variety of radionuclides with multiple photon energies. Sources with known activity should be placed around the detector and the resulting pulse height distribution unfolded. The photon flux at the detector should be calculated and compared with the value predicted by the unfolded spectra.

The effects of having relatively wide energy intervals (40 keV) on the accuracy of the unfolding process should be explored further. If the computational time can be significantly reduced as described above, a 10 keV interval might be warranted.

Finally, there are two factors that affect the measured pulse height distribution that need to be investigated: cosmic ray particles depositing some of their energy in the NaI(Tl) crystal, and the attenuation of low energy photons by the thin aluminum shield around the crystal. Once the contribution from these components has been defined, it would be simple to compensate for them during the unfolding routine.

LITERATURE CITED

Bevington, P.R. Data reduction and error analysis for the physical sciences. New York: McGraw-Hill; 1969.

Borak, T.B. Personal communication, 1988.

Knoll, G.F. Radiation detection and measurement. First printing. New York: John Wiley and Sons; 1979.

Grodstein, G.W. X-ray attenuation coefficients from 10 keV to 100 MeV. Washington DC: National Bureau of Standards Circular 583; 1957.

Harshaw Chemical Company. Harshaw scintillation phosphors, third edition. Solon, OH: Document #D-6589; 1975.

Hubbell, J.H. Response of a large sodium-iodide detector to high-energy γ-rays. Rev. Sci. Inst. 29:65-68; 1958.

Hubbell, J.H.; Gimm, H.A.; Overbo, I. Pair, triplet, and total atomic cross sections (and mass attenuation coefficients) for 1 MeV - 100 GeV photons in elements Z = 1 to 100. Journal of Physical Chemical Reference Data. 9:1023-1147; 1980.

Hubbell, J.H.; Veigele, Wm.J.; Briggs, E.A.; Brown, R.T.; Cromer, D.T. Atomic form factors, incoherent scattering functions and photon scattering cross sections. Journal of Physical Chemical Reference Data. 4:471-538;1975.

Merwin, S.E. An analytical model of the response of NaI(Tl) scintillation spectrometers to environmental gamma radiation. Master's Thesis. Colorado State University, Fort Collins, CO; 1985.

Wannigman, D.L. COWBOY operations on the CYBER 205. Unpublished report, 1989.

Whicker, J.J. A method to unfold environmental photon energy distribution from measured spectra. Master's Thesis. Colorado State University, Fort Collins, CO; 1988.

Zerby, C.D. A Monte Carlo calculation of the response of gamma-ray scintillation counters. In: Alder, B.; Fernbach, S.; Rotenburg, M., editors. Methods of mathematical physics. New York: Academic Press; 1963; 89-134.

APPENDIX

Energy dependent relationships for Compton and pair production cross sections used in computing the response functions. (E_γ = Photon energy in MeV)

Compton Cross Sections (cm^2/g)

For $E_\gamma \leq 0.001$ MeV: Cross section = 0.0

For $0.001 \text{ MeV} < E_\gamma \leq 0.005$ MeV:

$$\text{Cross section} = -0.00295 + (8.15 * E_\gamma) + (962 * E_\gamma^2) - (2.55E{+}05 * E_\gamma^3) + (1.66E{-}07 * E_\gamma^4)$$

$$R^2 = 1.00$$

For $0.005 \text{ MeV} < E_\gamma \leq 0.05$ MeV:

$$\text{Cross section} = 0.000611 + (9.59 * E_\gamma) - (353 * E_\gamma^2) + (6340 * E_\gamma^3) - (44000 * E_\gamma^4)$$

$$R^2 = 1.00$$

For $0.05 \text{ MeV} < E_\gamma \leq 1.0$ MeV:

$$\text{Cross section} = 0.123 - (0.102 * E_\gamma) - (0.109 * E_\gamma^2) + (0.300 * E_\gamma^3) - (0.159 * E_\gamma^4)$$

$$R^2 = 0.997$$

For $1.0 \text{ MeV} < E_\gamma \leq 5.0$ MeV:

$$\text{Cross section} = 0.0900 - (0.0503 * E_\gamma) + (0.0171 * E_\gamma^2) - (0.00293 * E_\gamma^3) + (0.000195 * E_\gamma^4)$$

$$R^2 = 1.00$$

Pair Production Cross Sections (cm^2/g)

For $E_\gamma < 1.022$ MeV: Cross section = 0.0

For $1.022 \leq E_\gamma < 5.0$ MeV:

$$\text{Cross section} = 2.13E\text{-}04 - [2.27E\text{-}03 * \ln(E_\gamma)] + [1.01E\text{-}02 * \ln(E_\gamma)^2] - [3.01E\text{-}03 * \ln(E_\gamma)^3] + [4.38E\text{-}04 * \ln(E_\gamma)^4]$$

$$R^2 = 1.00$$